Tailoring Fillet Weld Geometry Using a Genetic Algorithm and a Neural Network Trained with Convective Heat Flow Calculations

The combinations of welding variables needed to achieve a target gas metal arc fillet weld geometry can be systematically and quickly computed by a real-number-based genetic algorithm and a neural network

BY A. KUMAR AND T. DEBROY

ABSTRACT. A desired weld feature such as geometry can be produced using multiple sets of welding variables, i.e., different combinations of arc current, voltage, welding speed, and wire feed rate. At present, there is no systematic methodology that can determine, in a realistic time frame, these multiple paths based on scientific principles. Here we show that the various combinations of welding variables necessary to achieve a target gas metal arc (GMA) fillet weld geometry can be systematically and quickly computed by a real-number-based genetic algorithm and a neural network that has been trained with the results of a heat transfer and fluid flow model. The neural network is computationally efficient and, because of its origin, its input and the output obey the equations of conservation of mass, momentum, and energy. A genetic algorithm is used to determine a population of solutions by minimizing an objective function that represents the difference between the calculated and the desired values of the penetration, throat, and leg length. The model proposed here is different from traditional reverse models, since they cannot provide a choice of solutions and usually do not confirm to any phenomenological laws. The computational methodology provided a choice among various sets of current, voltage, welding speed, and wire feed rate for achieving a given fillet weld geometry specified by a set of leg length, penetration, and throat. The computed results were adequately verified by comparing with experimental results. The results provide hope that other weld attributes can also be tailored based on scientific principles in the future.

A. KUMAR and T. DEBROY are with Department of Materials Science and Engineering, The Pennsylvania State University, University Park, Pa.

Introduction

In recent years, phenomenological models of various fusion welding processes such as gas tungsten arc (Refs. 1–10), gas metal arc (GMA) (Refs. 11–16), and laser beam welding (Refs. 17–19) have been developed to better understand physical processes in welding and calculate the weld geometry (Refs. 3–10), cooling rate (Refs. 4, 11–13), and other weld attributes such as weld metal phase composition (Refs. 4, 8), grain structure (Refs. 5, 6), and inclusion structure (Ref. 7). Although these powerful models have provided significant insight about the effect of various welding variables, their applications have been rather limited (Refs. 20–22) for several reasons. First, the models are comprehensive and require a significant amount of computer time. Second, they are designed to calculate temperature and velocity fields for a given set of welding variables, i.e., they are unidirectional in nature. In other words, they cannot predict the welding variables needed to achieve a target weld geometry (Refs. 20–22) or other weld attributes. Finally, the GMA welding system is highly complex and involves nonlinear interaction of several welding variables (Refs. 11–16, 24). As a result, a particular weld attribute such as the geometry can be obtained via multiple paths, i.e., through the use of various sets of welding variables. What is very much needed, and not currently available, is for the models to have a capability to offer various choices of welding variable combinations, each capable of producing a target weld attribute. Traditional reverse models cannot produce multiple solutions and, in most instances, cannot confirm to any phenomenological laws.

KEYWORDS

Neural Networks
Gas Metal Arc Welding
Fillet Welds
Genetic Algorithm
Heat Transfer Models
Fluid Flow Models

Three main requirements need to be satisfied by a model for systematic tailoring of a weld attribute such as weld geometry based on scientific principles. First, the model should be capable of capturing all the major complex physical processes occurring during GMA welding. Second, the model must have a bidirectional capability. In other words, in addition to the capability of the traditional unidirectional, forward models to compute the weld shape and size from a given set of welding variables, it should also have the inverse modeling ability, i.e., it should be able to systematically predict welding variables needed to produce a target weld geometry. Finally, the model must be able to determine various welding variable sets needed to attain a target weld geometry within a reasonable time.

Since multiple paths can lead to a target weld geometry, the classical gradient-based search and optimization methods (Refs. 20–22) that produce a single optimum solution cannot be used. These methods use a point-by-point approach, where one relatively imperfect solution in

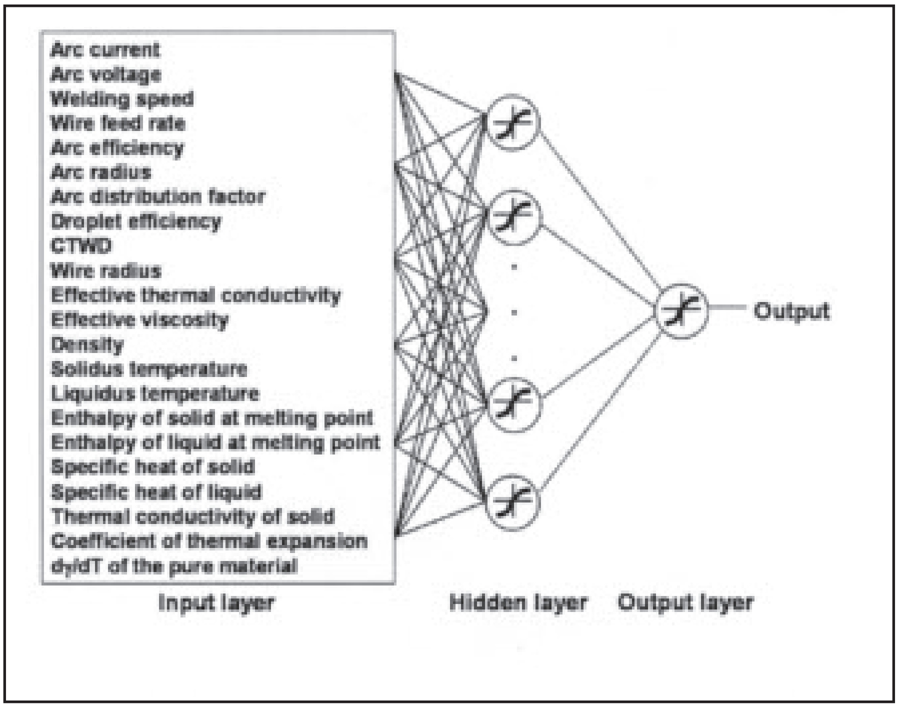

Fig. 1 — The architecture of the neural net model used in this work. The input layer is comprised of 22 variables. It is connected to a hidden layer. The output of the network is either penetration, leg length, or throat.

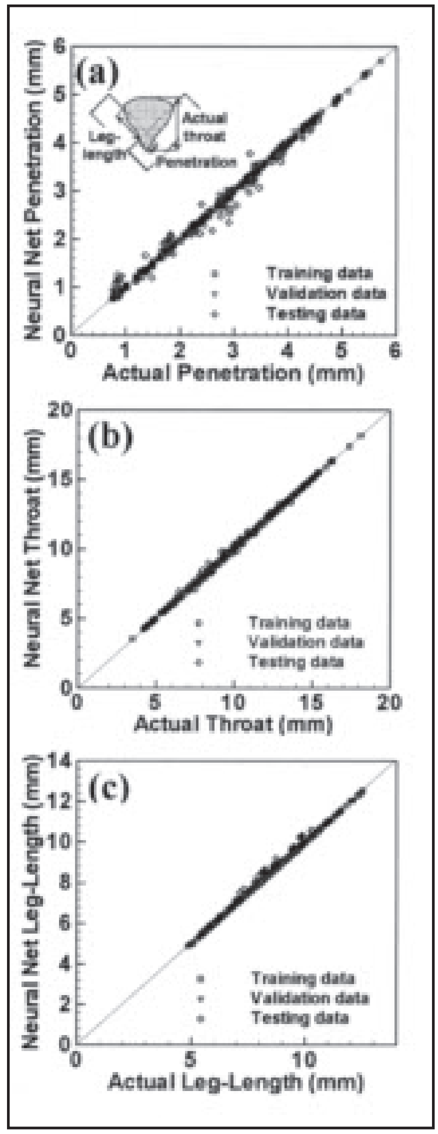

Fig. 2 — Comparison of output variables: A — Penetration; B — throat, calculated by heat transfer and fluid flow model (x axis) with corresponding values predicted by a neural network model of GMA fillet weld; C — leg length. The diagonal lines in each plot show that ideally all the points should lie on this line. The training data, validation data, and test data comprises 486, 50, and 25 datasets, respectively.

each iteration is modified to a different, more appropriate solution (Refs. 25, 26). Therefore, a combination of one of these classical optimization methods with the phenomenological model can provide only a single local optimum solution in situations where multiple solutions exist. In contrast, genetic algorithms (GA) mimic nature's evolutionary principles to derive its search toward a population of optimal solutions (Refs. 25–28). In the context of welding, a GA can systematically search for multiple combinations of welding variable sets that comply with the phenomenological laws of welding physics and improve with iterations (Refs. 20–22).

Recently, Kumar and DebRoy (Ref. 20) and Mishra and DebRoy (Refs. 21, 22) developed bidirectional phenomenological models of GMA fillet welding and GTA butt joint welding, respectively, by coupling a genetic algorithm-based optimization method with three-dimensional heat transfer and fluid flow model. They showed that the above approach can predict multiple combinations of welding variables to achieve a target geometry. However, these models (Refs. 20–22) are unsuitable for practical applications, since they require several days of computer calculations. Kumar and DebRoy (Ref. 20) used a parallel computing facility, i.e., running their model on multiple processors simultaneously to reduce computational time. Since it is very hard to maintain such a sophisticated computing facility in a manufacturing industry, their model can only be used for research purposes. Unless a model can do calculations in a reasonable time, it is unlikely to find widespread practical applications.

In gas metal arc welding, the effect of welding variables on the weld geometry is nonlinear and highly complex. A well-trained and rigorously tested neural network (Refs. 29–31) can be used in place of a phenomenological model to capture the correlations between different welding variables and weld attributes. The neural network models are able to predict the outputs for different welding conditions rapidly (Refs. 29–31). With the improvements in computational hardware in recent years, a large volume of training and validation data can be generated with a well-tested numerical heat transfer and fluid flow model in a realistic time frame. A neural network trained with the results of a numerical heat transfer and fluid flow model can correlate various output variables such as the weld pool geometry, cooling rate, liquid velocities, and peak temperatures with all the major welding variables and material properties. Furthermore, such correlations satisfy the basic scientific phenomenological laws expressed in the equations of conservation of mass, momentum, and energy.

We show here that multiple sets of welding variables that are capable of producing a target weld geometry can be calculated in a realistic time frame by coupling a genetic algorithm with a neural network model of gas metal arc fillet welding that has been trained with the results of a well-tested heat transfer and fluid flow model.

Mathematical Model

The main computational engine used here is a neural network model (Ref. 29), which is trained and validated using the results of a well-tested heat transfer and fluid flow model (Refs. 11–16). The neural network model includes all the welding variables and material properties as input and provides weld dimensions, peak temperatures, maximum velocities, and the

Table 1 — Terminology Used in Genetic Algorithm

Biological terms	Equivalent welding variables and representation in genetic algorithm
Genes: Units containing hereditary information	In the form of nondimensional variables, f_1, f_2, f_3, and f_4, e.g., f_1 = 1.10; f_2 = 1.70; f_3= 1.56; f_4 = 1.34.
Chromosome/individual: A number of genes folded together	A set of input variable values taken together, i.e., (1.10, 1.70, 1.56, 1.34)
Population: Collection of many chromosomes/ individuals	Collection of multiple sets: (1.10, 1.70, 1.56, 1.34), (1.20, 1.54, 1.65, 1.27), … … … … (1.23, 1.65, 1.75, 1.45)
Parents: Chromosomes/individuals participating for creating new individuals (or offsprings)	Parents: e.g., (1.10, 1.70, 1.56, 1.34), (1.23, 1.65, 1.75, 1.45)
Objective function value: Value of objective function determines if a chromosome/individual survives or dies	Objective function: Calculated for each set of input variables using Equation 2.

cooling rates between 800° and 500°C. This network has 22 input parameters that are connected to output layer through a hidden layer of 19 nodes as shown in Fig. 1. A hyperbolic tangent function (which is a symmetric sigmoid function) is used as the activation function to include nonlinear behavior of different variables. A back-propagation algorithm (Refs. 29, 33–35) was used to update the synaptic weights of the neural network. The algorithm used a hybrid method involving a genetic algorithm and a conjugate gradient technique to reduce the least square error, E, between the actual outputs (d) and predicted values (y) (Ref. 29):

$$E=\frac{1}{2}\sum_{p}\left(d_o^{(p)}-y_o^{(p)}\right)^2 \tag{1}$$

where *p* represents the number of training datasets and *o* represents the number of output nodes, which is one in this work. The hybrid algorithm reduces the training time as the conjugate gradient method takes advantage of gradient information to calculate the optimal solution, whereas the genetic algorithm helps to avoid local minima (Ref. 29). The resulting neural network is computationally more efficient than a phenomenological heat transfer and fluid flow model. Furthermore, the results from the neural network model matches the corresponding results from the heat and fluid flow model.

The genetic algorithm-based search for multiple sets of welding variables to achieve a target weld geometry starts with many initial sets of randomly chosen values of the four most important welding variables, i.e., current, voltage, welding speed, and the wire feed rate. A systematic global search is next undertaken to find multiple sets of values of these four welding variables that lead to least error between the calculated and the target weld dimensions, i.e., penetration, throat, and leg length. The neural network model calculates the values of these weld dimensions for each set of input welding variables. The chosen values of welding variables do not always produce the desired weld dimensions and the resulting mismatch between the computed and the desired weld dimensions is expressed by the following objective function, O(f):

$$O(f)=\left(\frac{p^c}{p^t}-1\right)^2+\left(\frac{t^c}{t^t}-1\right)^2+\left(\frac{l^c}{l^t}-1\right)^2 \tag{2}$$

where p^c, t^c, and l^c are the computed penetration, throat, and leg length of the weld bead, respectively, and p^t, t^t, and l^t are the corresponding target or desired values of these three parameters. The objective function, O(f), depends on four main welding variables, i.e., current, I, voltage, V, welding speed, U, and the wire feed rate, w_f.

$$O(f)=O\left(f_1,f_2,f_3,f_4\right)=O\left(\frac{I}{I_r},\frac{V}{V_r},\frac{U}{U_r},\frac{w_f}{\left(w_f\right)_r}\right) \tag{3}$$

In Equation 3, the reference values, I_r, V_r, U_r, and $(w_f)_r$ represent the order of magnitude of the welding variables. Note that Equation 3 is made nondimensional to preserve the importance of all four welding variables by making their nondimensional values comparable in magnitude. The GA produces new individuals, or sets of welding conditions, with iterations based on the evolutionary principles (Refs. 20–22, 26–28) as explained in the Appendix. Table 1 provides the explanation of various terminology used in GA related to welding.

Genetic algorithms work with a set of "individuals," a population where each individual is a solution of a given problem. The initial population defines the possible solutions of the optimization problem, i.e., sets of welding variables that completely define a weld such as current, voltage, welding speed, contact tube-to-workpiece distance, and wire feed rate. There are two popular ways of representing the variables in the population in GA: binary and real numbers. Generally, binary representation of variables converges slowly compared to the real representations. In addition, since the binary genetic algorithm has its precision limited by the binary representation of variables, using real numbers allows representation to the machine precision. The real coded genetic algorithm also has the advantage of requiring less storage than the binary GA because a single floating point number represents a variable instead of many integers having values 0 and 1. The other important advantage of using real coded GA is its accuracy and precision in representing the variables in continuous search space.

The genetic algorithm (GA) used in the present study is a parent centric recombination (PCX) operator-based generalized generation gap (G3) model (Refs. 20–22, 27–29). The generic parent-centric recombination operator (PCX) is an elite-preserving, scalable, and computationally fast population-alteration model (Ref. 27). This model was chosen because it has been shown to have a faster convergence rate on standard test functions as compared to other evolutionary algorithms and classical optimization algorithms including other real-parameter GAs with the unimodal normal distribution crossover (UNDX) and the simplex crossover (SPX) operators, the correlated self-adaptive evolution strategy, the covariance matrix adaptation evolution strategy (CMA-ES), the differential evolution technique, and the quasi-Newton method (Ref. 27). The original G3 model applied by Kumar et al. (Ref. 28), Kumar and DebRoy (Ref. 20), and Mishra and DebRoy (Refs. 21, 22) for different welding applications has very high selectivity, since at every iteration individuals are created using the best parent and two randomly chosen individuals. The high selec-

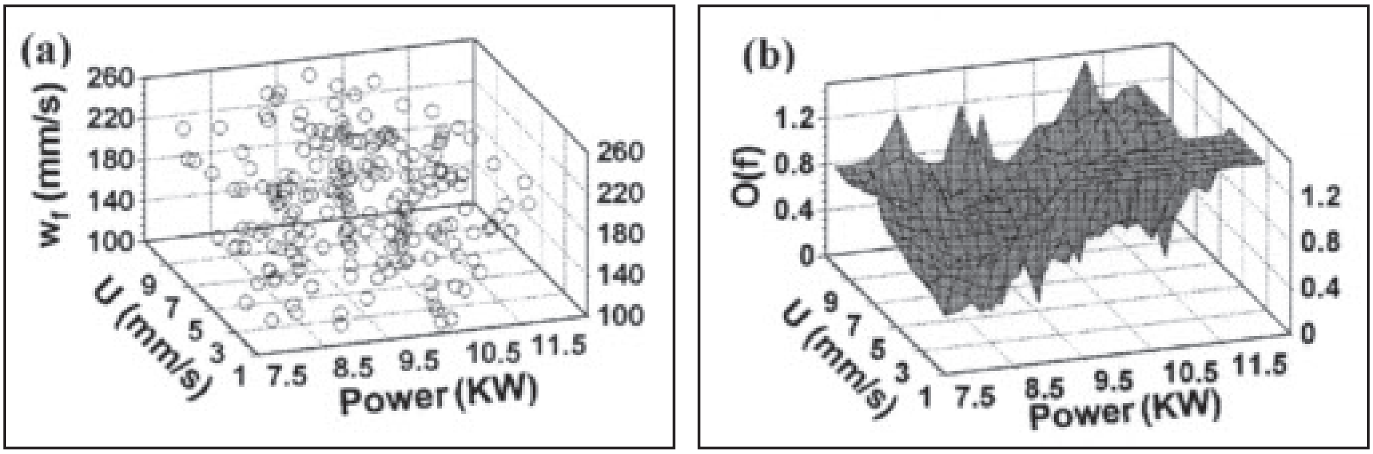

Fig. 3 — Initial values of individual welding variable sets and their objective functions. A — A large space of variables was searched to find optimum solutions as shown by 200 randomly selected initial welding variable sets; and B — the low values of the objective functions of several individuals in the initial population indicate the possibility of existence of multiple optimal solutions.

tivity tends to draw the whole population of solutions toward one side of the parameter space. In order to maintain diversity in the population, a modified version of the generalized generation gap (G3) model is used in this work. Here we use three randomly chosen parents to create new individuals in place of best parent and two randomly chosen individuals in the original algorithm.

Results and Discussion

The neural network used here was trained and validated with results from a well-tested three-dimensional numerical heat transfer and fluid flow model. A large database of outputs for different welding conditions was generated based on design of experiments (DOE) (Ref. 29) to capture the correlations between the welding variables and the weld attributes. Separate feed-forward neural networks were developed, one each for predicting penetration, leg length, and throat of a GMA fillet weld in spray mode to achieve high accuracies in the calculation of penetration, leg length, and throat. The weights in the neural network models were calculated using a hybrid optimization scheme involving the conjugate gradient (CG) method and a genetic algorithm (GA). The network was trained using only the training data. The validation and testing data were randomly generated independent of the training data. The performance of the network was tested using the validation and testing datasets. The testing data were used to check the overall performance of the network. The hybrid optimization scheme helped in finding optimal weights through a global search as evidenced by good agreement between all the outputs from the neural networks and the corresponding results from the heat and fluid flow model as shown in Fig. 2. These results are obtained for welding of A-36 steel plates using argon with 10% CO_2 as shielding gas and solid feed wire of 1.32-mm diameter. The droplet transfer mechanism during welding is assumed to be in spray mode. The workpiece was 450 mm in length, 108 mm in width, and 18 mm in depth. The nominal composition of A-36 steel is maximum 0.29% C, 0.80–1.2% Mn, 0.04% P, 0.05% S, 0.15–0.3% Si, and remaining percentage of Fe. The neural network model provided correct values of penetration, actual throat, and leg length for various combinations of welding variables I, V, U, and w_f as shown in Fig. 2. Since GA can provide a population of solutions, the neural network model must be combined with an appropriate GA to tailor weld attributes.

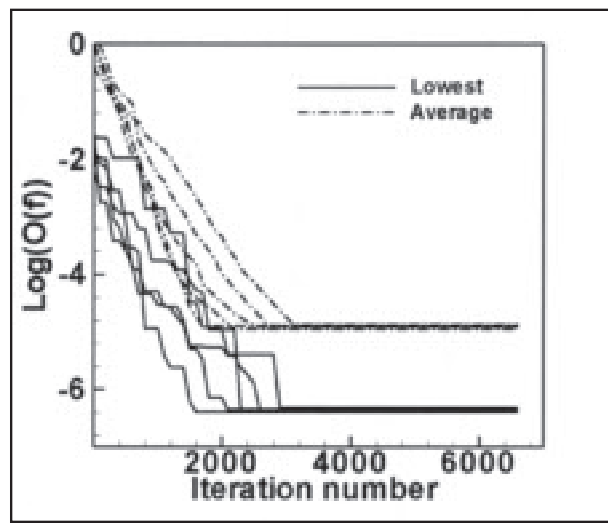

Fig. 4 — Variation of the minimum value and the average value of the objective function in whole population with iterations for 5 different randomly selected initial populations. The low value of the objective function shows that the converged solution is independent on initial selection of values of individuals in the population.

The effectiveness of the model proposed here was tested by finding different sets of welding variables that could provide a specified weld geometry based on scientific principles. The computational task involved three steps. First, a target weld geometry was selected by specifying one set of values of penetration, throat, and leg length. Second, the model was run to obtain multiple combinations of welding variable sets each of which could produce the target weld geometry. Third, and final, the results obtained from the model were adequately verified. These three steps are explained in detail in the next section.

To start the calculation, the specification of a target geometry was necessary. It involved stating realistic combinations of the three weld dimensions, i.e., penetration, throat, and leg length. To test the model, these three weld dimensions from an actual welding experiment were specified as a target geometry. If the model works correctly, the various combinations of welding variables obtained from the model must include a set of welding variables that are fairly close to the set of variables used in the experiment. It should be noted that the ability of the model to produce this solution is only a necessary, but not sufficient, component of the model verification. Since the model produced multiple solutions, other solutions obtained from the model had to be verified by comparing the calculated weld geometry

Table 2 — The Various Combinations of Welding Parameters, i.e., Arc Current (I), Arc Voltage (V), Welding Speed (U), and Wire Feed Rate (w_f) Obtained Using Neural Network Model to Achieve the Following Target Weld Dimensions: Penetration = 1.6 mm, Leg Length = 10.5 mm, and Throat = 7.2 mm. The Target Weld Geometry Was Obtained Experimentally Using the Following Welding Variables: I = 286.8 A, V= 33.0 V, U = 4.2 mm/s, and w_f = 169.3 mm/s.

Individual Solutions	I (Amp)	V (Volt)	U (mm/s)	w_f (mm/s)	Penetration (mm)	Leg Length (mm)	Throat (mm)
(a)	285.1	33.1	4.2	172.4	1.7	10.5	7.2
(b)	293.3	32.6	4.3	211.0	1.6	10.6	7.1
(c)	298.3	31.3	4.5	216.2	1.6	10.5	7.2
(d)	290.8	33.5	4.6	210.0	1.6	10.5	7.2
(e)	292.2	33.0	4.6	213.0	1.6	10.5	7.1
(f)	303.3	30.6	4.6	210.5	1.6	10.3	7.3
(g)	294.1	31.4	4.9	227.0	1.6	10.5	7.2
(h)	294.7	31.0	5.0	231.0	1.6	10.5	7.2

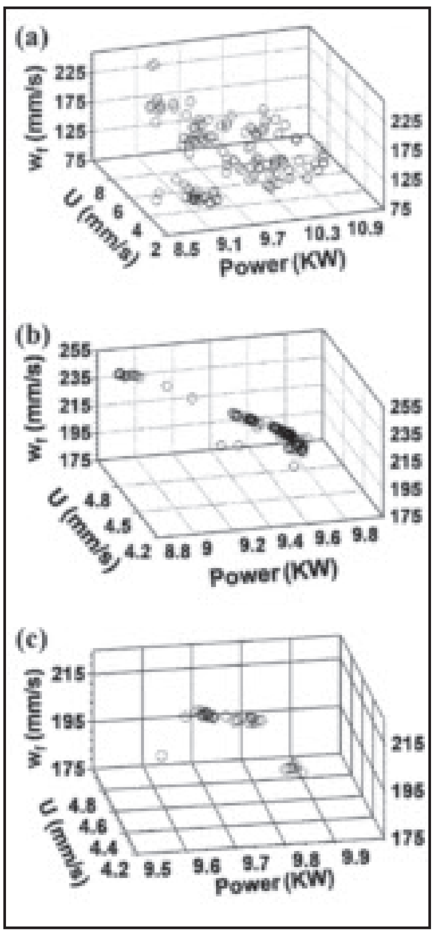

Fig. 5 — Several fairly diverse welding variable sets could produce low values of the objective function indicating the existence of alternate paths to obtain the target weld geometry. The plots show the welding variable sets that produced low values of the objective function, O(f) with iterations. A — Individuals after 1000 iterations with O(f) less than 1 × 10^{-2}; B — individuals after 3000 iterations with O(f) less than 1 × 10^{-4}; and C — individuals after 6000 iterations with O(f) less than 1 × 10^{-5}.

with the experimentally obtained geometry.

In the next step (i.e., second step), a population of 200 individuals was defined to start the operation of GA. Each individual in the population defined a set of randomly chosen welding variables such as current, voltage, welding speed, and wire feed rate. Choice of an appropriate population size was important. A small population size did not allow adequate representation of the variable space. On the other hand, a very large population size resulted in large computational volume. For example, Fig. 3A depicts the initial values of the individuals, i.e., sets of I, V, U, and w_f of each individual solution with I and V plotted as their product in the form of input arc power. Values of the welding variables I, V, U, and w_f were chosen randomly in the range of 250–400 A, 27–35 V, 3.5–7.0 mm/s, and 150–250 mm/s, respectively. The values of the welding variables in such large ranges helped in maintaining diversity in the solutions. These welding variable sets were then improved iteratively using a combination of GA and the neural network. With the progress in the calculations, the average objective function values decreased with iterations. An individual with a low objective function indicates correct combinations of current, voltage, welding speed, and wire feed rate that can result in the target weld geometry. Figure 3B shows the computed values of the objective functions for all the individuals depicted in Fig. 3A. This figure shows that for many sets of welding variables, the values of the objective function, O(f), were fairly low indicating that each of these welding variable sets could produce a weld geometry that was close to the target geometry.

Figure 4 shows that the objective function decreased rapidly with iterations for the best individual whereas the average value of the objective function of the whole population decreased at a relatively slower pace. This behavior is consistent with the fact that as GA tries to explore the solution space, it produces new sets of welding parameters that has high values of O(f).

Figure 5A indicates several individuals with objective function values lower than 0.01 corresponding to the 1000th generation or iteration. With the increase in number of iterations the diversity of population decreases, and the solution starts crowding in different regions. Figure 5B and C shows the individual solutions with objective function values less than 1 × 10^{-4} and 1 × 10^{-5} at generations 3000 and 6000, respectively. The calculation is continued until 5% of individuals in the population have the value of objective function less than 1.0 × 10^{-6}. The chosen value of the objective function (fitness) ensured sufficient accuracy within the practical limits of the experimental errors. The calculated combinations of the welding variables are presented in Table 2. The calculations required less than one minute in a PC with 3.2 GHz Intel P4 CPU and 1024 Mb PC2700 DDR-SDRAM memory. It is useful to recall that several days of computational time were required on multiple processors by a model developed by Kumar and DebRoy (Ref. 20) that used a numerical heat transfer and fluid flow model. This time saved by using a neural network justifies its use as a forward model in place of a heat transfer and fluid flow model.

The third step involved verification of the computed solutions. Since the target geometry was produced by conducting an experiment, an initial test is to check if the population of solutions produced by the model include a set of welding variables that is very close to, if not the same as, that used to produce the weld. Solution (a) in Table 2 involves welding parameters that are very close, within less than 1%, to those used to produce the experimental weld. This table also includes values of other variable sets, i.e., current, voltage, welding speed, and wire feed rate, computed by the model to produce the desired values of leg length, penetration, and throat. Each solution, i.e., a set of current, voltage, welding speed, and wire feed rate was used to calculate weld geometric parameters. The computed geometric parameters were then compared with those produced in the experiment. Table 2 shows that for each set of computed welding con-

Table 3 — The Various Combinations of Welding Parameters, i.e., Arc Current (I), Arc Voltage (V), Welding Speed (U), and Wire Feed Rate (w_f) Obtained Using Neural Network Model to Achieve the Following Target Weld Dimensions: Penetration = 3.7 mm, Leg Length = 12.0 mm, and Throat = 10.0 mm. The Target Weld Geometry Was Obtained Using the Welding Conditions Listed in (a).

Individual Solutions	I (Amp)	V (Volt)	U (mm/s)	w_f (mm/s)	Penetration (mm)	Leg Length (mm)	Throat (mm)
(a)	301.6	34.6	3.4	228.6	3.7	12.0	10.0
(b)	306.2	34.6	3.6	236.6	3.7	12.0	10.0
(c)	300.3	34.6	3.3	225.9	3.7	12.0	10.0
(d)	311.0	35.3	4.5	270.8	3.7	12.0	10.0
(e)	290.8	35.4	4.1	260.2	3.7	12.0	10.0
(f)	314.1	33.5	3.8	239.0	3.7	11.8	10.0

ditions, the corresponding geometric parameters agreed well with the desired experimental values.

A similar exercise was also undertaken where a hypothetical weld geometry represented by a leg length of 12 mm, penetration of 3.7 mm, and throat of 10 mm were produced by a 301.6-A current, 34.6-V voltage, 3.4-mm/s welding speed, and 228.6-mm/s wire feed rate. Table 3 lists all other combinations of welding variables i.e., solutions (b) to (f), that can also produce this geometry. The values of the welding variables differ considerably from each other. For example, the current, wire feed rate, and welding speed vary among solutions by 8%, 20%, and 36%, respectively. It should be noted that very often the dimensions of the weld vary by 1 to 2 mm; if we allow that much variation, then leg length = 10.6 mm, throat = 10.1 mm, and penetration = 3.6 mm can be obtained using I = 417.5 amps, V = 37.5 volts, U = 6.7 mm/s, and w_f = 234.0 mm/s. All these differences in the important welding variables indicate significant diversity in the paths, all of which lead to the same set of target weld dimensions.

The rapid computational methodology involving a neural network and a genetic algorithm described here enables realistic tailoring of GMA fillet weld geometry based on scientific principles for the first time. The model computes practical choices of alternative paths involving multiple combinations of welding variables to achieve a desired weld geometry in less than a minute with a commonly available PC. It is hoped that the methodology will serve as basis for formulating, testing, and implementing realistic computational tools for tailoring weld attributes to achieve defect free, structurally sound, and reliable welds.

Conclusions

Unlike conventional heat transfer and fluid flow models that can predict weld geometry for a particular set of welding conditions, a new model has been developed that can calculate alternative welding conditions needed to obtain a target weld geometry. The model developed is significantly different from traditional reverse models that provide only one set of welding conditions necessary for obtaining a target weld geometry. In reality, a particular weld geometry can be obtained by using various combinations of welding variables and the new model can calculate these alternative pathways. The model combines a neural network model of heat and fluid flow with a real-number-based genetic algorithm to calculate alternative welding conditions needed to obtain a target weld geometry for GMA fillet welding. The use of a neural network model in place of a heat transfer and fluid flow model significantly increased computational efficiency and provided multiple solutions within one minute in a commonly available computer.

The model was used to determine multiple sets of welding variables, i.e., combinations of welding current, voltage, speed, and wire feeding rate to obtain a specified weld pool geometry. It was found that a specific weld geometry was attainable via multiple pathways involving various sets of welding variables. Furthermore, these sets of welding variables involved significantly different values of current, voltage, welding speed, and wire feed rate. Good agreement between the model predictions and the experimental data of leg length, penetration, and throat for various welding conditions shows that this approach is promising for practical shop floor applications. Although the work reported here focuses on tailoring weld geometry, the results provide hope that science-based tailoring of structure and properties of weldments may also become attainable in the future.

Acknowledgments

This research was supported by a grant from the U.S. Department of Energy, Office of Basic Energy Sciences, Division of Materials Sciences, under grant number DE-FGO2-01ER45900. Mr. Kumar gratefully acknowledges award of a Fellowship in the American Welding Society.

Appendix: PCX-Based G3 Genetic Algorithm

The genetic algorithm used in the present study is a parent centric recombination (PCX) operator-based generalized generation gap (G3) model (Refs. 20–22, 27, 28). The steps involved in the calculations are as follows:

1. A population is a collection of many individuals and each individual represents a set of randomly chosen values of the four nondimensionalized welding variables. A parent refers to an individual in the current population. The best parent is the individual that has the best fitness, i.e., gives the minimum value of the objective function, defined by Equation 2 in the main text, in the entire population. Three parents are chosen randomly from the population of solutions.

2. From the three randomly chosen parents, two offsprings or new individuals are generated using a recombination scheme. PCX-based G3 models are known to converge rapidly when three parents and two offsprings are selected (Ref. 27). A recombination scheme is a process for creating new individuals from the parents.

3. Two new parents are randomly chosen from the current population of the individuals.

4. A subpopulation of four individuals that includes the two randomly chosen parents in step 3 and two new offsprings generated in step 2 is formed.

5. The two best solutions, i.e., the solutions having the least values of the objective function, are chosen from the subpopulation of four members created in step 4. These two individuals replace the two parents randomly chosen in step 3.

6. The calculations are repeated from step one again until convergence is achieved.

The above steps, as applied to the present problem, are shown in Fig. 6. Figure 7 illustrates the working of the model to find the window of welding parameters to achieve a target weld geometry. The recombination scheme (step 2) used in the

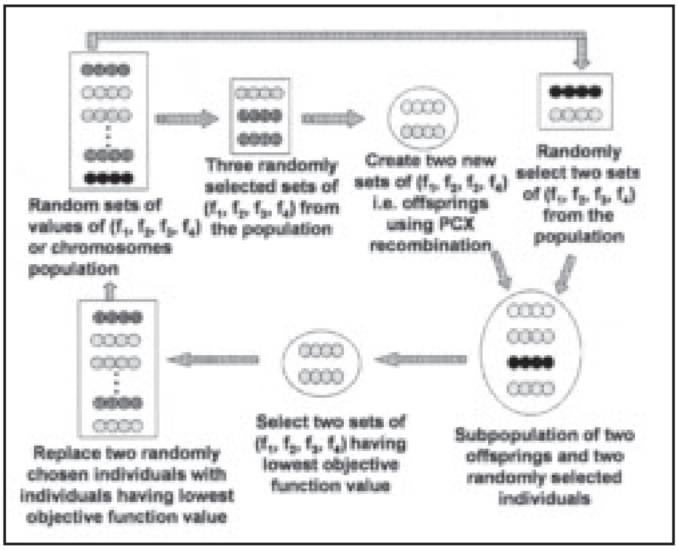

Fig. 6 — The working principle of the genetic algorithm based on generalized generation gap (G3) model and using parent centric recombination (PCX) operator.

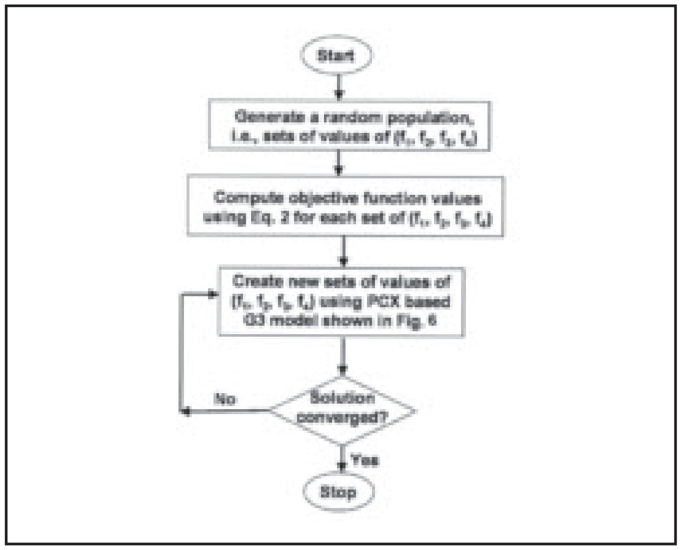

Fig. 7 — Flow chart of the proposed model after coupling of generalized generation gap (G3) genetic algorithm with neural network model.

present model is based on a parent centric recombination (PCX) operator (Refs. 20–22, 27, 28). A brief description of this operator, as applied to the present problem, is presented below:

First three parents, i.e.,

$$\left(f_1^0, f_2^0, f_3^0, f_4^0\right),\ \left(f_1^1, f_2^1, f_3^1, f_4^1\right),\ \left(f_1^2, f_2^2, f_3^2, f_4^2\right),$$

are randomly selected from the current population. Here the subscripts represent the four variables or the welding parameters, while the superscripts denote the parent identification number. The mean vector or centroid,

$$\vec{g} = \begin{pmatrix} \dfrac{f_1^0+f_1^1+f_1^2}{3}, \dfrac{f_2^0+f_2^1+f_2^2}{3}, \\ \dfrac{f_3^0+f_3^1+f_3^2}{3}, \dfrac{f_4^0+f_4^1+f_4^2}{3} \end{pmatrix},$$

of the three chosen parents is computed. To create an offspring, one of the parents, say

$$\vec{x}^{(p)} = \left(f_1^0, f_2^0, f_3^0, f_4^0\right),$$

is chosen randomly. The direction vector, $\vec{d}^{(p)} = \vec{x}^{(p)} - \vec{g}$ is next calculated from the selected parents to the mean vector or centroid. Thereafter, from each of the other two parents, i.e.,

$$\left(f_1^1, f_2^1, f_3^1, f_4^1\right), \text{ and } \left(f_1^2, f_2^2, f_3^2, f_4^2\right)$$

perpendicular distances, D_i, to the direction vector, $\vec{d}^{(p)}$, are computed and their average, $\overline{D}$, is found. Finally, the offspring i.e., $\vec{y} = \left(f_1', f_2', f_3', f_4'\right)$, is created as follows:

$$\vec{y} = \vec{x}^{(p)} + w_\zeta \left|\vec{d}^{(p)}\right| + \sum_{i=1, i\neq p}^{4} w_\eta \overline{D}\vec{h}^{(i)} \quad \text{(A.1)}$$

where $\bar{h}^{(i)}$ are the orthonormal bases that span the subspace perpendicular to $\bar{d}^{(p)}$, and w_ζ and w_η are randomly calculated zero-mean normally distributed variables. The values of the variables that characterize the offspring,

$$\vec{y} = \left(f_1', f_2', f_3', f_4'\right),$$

are calculated as follows:

$$f_1' = f_1^0 + f_{11} + f_{12} \quad \text{(A2.a)}$$

$$f_2' = f_2^0 + f_{21} + f_{22} \quad \text{(A2.b)}$$

$$f_3' = f_3^0 + f_{31} + f_{32} \quad \text{(A2.c)}$$

$$f_4' = f_4^0 + f_{41} + f_{42} \quad \text{(A2.d)}$$

where,

$$f_{11} = w_\zeta \left(\frac{2f_1^0 - f_1^1 - f_1^2}{3}\right) \quad \text{(A3.a)}$$

$$f_{21} = w_\zeta \left(\frac{2f_2^0 - f_2^1 - f_2^2}{3}\right) \quad \text{(A3.b)}$$

$$f_{31} = w_\zeta \left(\frac{2f_3^0 - f_3^1 - f_3^2}{3}\right) \quad \text{(A3.c)}$$

$$f_{41} = w_\zeta \left(\frac{2f_4^0 - f_4^1 - f_4^2}{3}\right) \quad \text{(A3.d)}$$

$$f_{12} = w_\eta \left(\frac{a_2 + b_2}{2}\right) \left[1 - \left(\frac{2f_1^0 - f_1^1 - f_1^2}{3d}\right)^2\right] \quad \text{(A3.e)}$$

$$f_{22} = w_\eta \left(\frac{a_2 + b_2}{2}\right) \left[1 - \left(\frac{2f_2^0 - f_2^1 - f_2^2}{3d}\right)^2\right] \quad \text{(A3.f)}$$

$$f_{32} = w_\eta \left(\frac{a_2 + b_2}{2}\right) \left[1 - \left(\frac{2f_3^0 - f_3^1 - f_3^2}{3d}\right)^2\right] \quad \text{(A3.g)}$$

$$f_{42} = w_\eta \left(\frac{a_2 + b_2}{2} \right) \left[1 - \left(\frac{2f_4^0 - f_4^1 - f_4^2}{3d} \right)^2 \right] \quad \text{(A3.h)}$$

The various unknown variables used in Equations A3.a to A3.h can be represented in simplified form as follows:

$$d = \sqrt{\left(\frac{2f_1^0 - f_1^1 - f_1^2}{3} \right)^2 + \left(\frac{2f_2^0 - f_2^1 - f_2^2}{3} \right)^2 + \left(\frac{2f_3^0 - f_3^1 - f_3^2}{3} \right)^2 + \left(\frac{2f_4^0 - f_4^1 - f_4^2}{3} \right)^2} \quad \text{(A4.a)}$$

$$a_2 = e_1 \times \sqrt{1 - (a_1)^2} \quad \text{(A4.b)}$$

$$b_2 = e_2 \times \sqrt{1 - (b_1)^2} \quad \text{(A4.c)}$$

$$a_1 = \sum_{i=1}^{i=4} \frac{\left(f_i^1 - f_i^0 \right) \left(\frac{2f_i^0 - f_i^1 - f_i^2}{3} \right)}{d \times e_1} \quad \text{(A4.d)}$$

$$e_1 = \sqrt{\left(f_1^1 - f_1^0 \right)^2 + \left(f_2^1 - f_2^0 \right)^2 + \left(f_3^1 - f_3^0 \right)^2 + \left(f_4^1 - f_4^0 \right)^2} \quad \text{(A4.e)}$$

$$b_1 = \sum_{i=1}^{4} \frac{\left(f_i^2 - f_i^0 \right) \left(\frac{2f_i^0 - f_i^1 - f_i^2}{3} \right)}{d \times e_2} \quad \text{(A4.f)}$$

$$e_2 = \sqrt{\left(f_1^2 - f_1^0 \right)^2 + \left(f_2^2 - f_2^0 \right)^2 + \left(f_3^2 - f_3^0 \right)^2 + \left(f_4^2 - f_4^0 \right)^2} \quad \text{(A4.g)}$$

References

1. David, S. A., and DebRoy, T. 1992. Current issues and problems in welding science. *Science* 257: 497–502.

2. DebRoy, T., and David, S. A. 1995. Physical processes in fusion welding. *Reviews of Modern Physics* 67(1): 85–112.

3. Kumar, A., and DebRoy, T. 2003. Calculation of three-dimensional electromagnetic force field during arc welding. *Journal of Applied Physics* 94(2): 1267–1277.

4. Zhang, W., Elmer, J. W., and DebRoy, T. 2002. Rate of ferrite to austenite transformation during heating of 1005 steel. *Scripta Materialea* 46(10): 753–757.

5. Mishra, S., and DebRoy, T. 2004. Grain topology in Ti-6Al-4V welds — Monte Carlo simulation and experiments. *Journal of Physics D: Applied Physics* 37: 2191–2196.

6. Mishra, S., and DebRoy, T. 2003. Measurements and Monte Carlo simulation of grain structure in the heat-affected zone of Ti-6Al-4V welds. *Acta Materialia* 52(5): 1183–1192.

7. Hong, T., and DebRoy, T. 2003. Nonisothermal growth and dissolution of inclusions in liquid steels. *Metallurgical and Materials Transactions B* 34: 267–269.

8. De, A., and DebRoy, T. 2004. A smart model to estimate effective thermal conductivity and viscosity in weld pool. *Journal of Applied Physics* 95(9): 5230–5239.

9. De, A., and DebRoy, T. 2004. Probing unknown welding parameters from convective heat transfer calculation and multivariable optimization. *Journal of Physics D: Applied Physics* 37: 140–150.

10. De, A., and DebRoy, T. 2005. Reliable calculations of heat and fluid flow during conduction mode laser welding through optimization of uncertain parameters. *Welding Journal* 84(7): 101–112.

11. Kim, C. H., Zhang, W., and DebRoy, T. 2003. Modeling of temperature field and solidified surface profile during gas metal arc fillet welding. *Journal of Applied Physics* 94: 2667–2679.

12. Zhang, W., Kim, C. H., and DebRoy, T. 2004. Heat transfer and fluid flow in welds with complex geometry during gas-metal-arc fillet welding, Part I: Numerical model. *Journal of Applied Physics* 95: 5210–5219.

13. Zhang, W., Kim, C. H., and DebRoy, T. 2004. Heat transfer and fluid flow in welds with complex geometry during gas-metal-arc fillet welding, Part II: Application to fillet welding of mild steel. *Journal of Applied Physics* 95: 5220–5229.

14. Kumar, A., and DebRoy, T. 2004.Guaranteed fillet weld geometry from heat transfer model and multivariable optimization. *International Journal of Heat and Mass Transfer* 47(26): 5793–5806.

15. Kumar, A., and DebRoy, T. 2005. Improving reliability of modeling heat transfer and fluid flow in gas-metal-arc fillet welding – Part II: Application to welding of steel. *Journal of Physics D: Applied Physics* 38: 127-134.

16. Kumar, A., Zhang, W., and DebRoy, T. 2005. Improving reliability of modeling heat transfer and fluid flow in gas-metal-arc fillet welding — Part II: An engineering physics model. *Journal of Physics D: Applied Physics* 38: 119–126.

17. He, X., Fuerschbach, P., and DebRoy, T. 2004. Composition change of stainless steel during micro-joining with short laser pulse. *Journal of Applied Physics* 96(8): 4547–4555.

18. He, X., Fuerschbach, P., and DebRoy, T. 2003. Heat transfer and fluid flow during laser spot welding of 304 stainless steel. *Journal of Physics D: Applied Physics* 36: 1388–1398.

19. Zhao, H., and DebRoy, T. 2003. Macroporosity free aluminum alloy weldments through numerical simulation of keyhole mode laser welding. *Journal of Applied Physics* 93(12): 10089–10096.

20. Kumar, A., and DebRoy, T. 2005. Tailoring complex weld geometry through reliable heat transfer and fluid flow calculations and a genetic algorithm. *Metallurgical and Materials Transaction A-Physical Metallurgy and Material Science* 36 A(10): 2725–2735.

21. Mishra, S., and DebRoy, T. 2005. A computational procedure for finding multiple solutions of convective heat transfer equation. *Journal of Physics D* 38: 2977–2985.

22. Mishra, S., and DebRoy, T. 2005. A heat transfer and fluid flow based model to obtain a specific weld geometry through multiple paths. *Journal of Applied Physics* 98: 044902.

23. Fuerschbach, P. W., and Eisler, G. R. 2002. Effect of laser spot weld energy and duration on melting and absorption. *Science and Technology of Welding and Joining* 7(4): 241–246.

24. Smartt, H. B., and Einerson, C. J. 1993. A model for heat and mass input control in GMAW. *Welding Journal* 72(5): 217–229.

25. Goldberg, D. E. 1989. *Genetic Algorithm in Search, Optimization and Machine Learning*. Addison-Wesley, Mass., pp. 25–74.

26. Deb, K. 2001. Multi-objective Optimization Using Evolutionary Algorithms. New York, N.Y.: Wiley.

27. Deb, K., Anand, A., and Joshi, D. 2002. A computationally efficient evolutionary algorithm for real-parameter optimization. *Evolutionary Computation* 10: 371–395.

28. Kumar, A., Mishra, S., Elmer, J. W., and DebRoy, T. 2005. Optimization of Johnson Mehl Avarami equation parameters for α-ferrite to γ-austenite transformation in steel welds using a genetic algorithm. *Metallurgical and Material Transaction A* 36: 15–22.

29. Kumar, A., and DebRoy, T. 2006. A neural network model of heat and fluid flow in gas metal arc fillet welding based on genetic algorithm and conjugate gradient optimization. *Science and Technology of Welding and Joining* 11(1): 106–119.

30. Vitek, J. M., Iskander, Y. S., and Oblow, E. M. 2000. Improved ferrite number prediction in stainless steel arc welds using artificial neural networks — Part 1: Neural network development. *Welding Journal* 79(2): 33–40.

31. Bhadeshia, H. K. D. H. 1999. Neural networks in materials science. *ISIJ International* 39 (10): 966-979.

32. Patankar, S. V. 1980. *Numerical Heat Transfer and Fluid Flow.* New York, N.Y.: Hemisphere. pp. 41–71.

33. Haykin, S. 1999. *Neural Network: A Comprehensive Foundation.* Prentice Hall Pub., N.J., pp. 156–234.

34. Masters, T. 1993. *Practical Neural Network Recipes in C++*. Boston, Mass.: Academic Press.

35. Hagan, M. T. 1996. *Neural Network Design.* Boston, Mass.: PWS Pub.